Ground Vibration Tests on a Flexible Flying Wing Aircraft

Abhineet Gupta* and Peter Seiler†

University of Minnesota, Minneapolis, MN 55455, USA

Brian Danowsky‡

Systems Technology Inc., Hawthorne, CA 90250, USA

This paper presents ground vibration test results for a small flexible flying wing aircraft. The aircraft is suspended from a spring and an input force is applied via an electrodynamic shaker. Accelerometer measurements are obtained at twenty points along the aircraft wings. This measured force and acceleration data is post-processed to identify modal frequencies and mode shapes using two different methods. The effect of small changes in the experimental procedure on the identified modal parameters is discussed. The tests were performed on a series of flexible aircraft that were built to study flutter and other aeroelastic phenomena.

I. Introduction

More fuel efficient aircraft can be designed by reducing structural weight and incorporating advanced light-weight materials. A drawback of such designs is an increase in the aircraft flexibility, resulting in large deformations under loading. Moreover, the frequencies of the flexible modes decrease. As a result, the flexible modes can start interacting with the rigid body modes. This can degrade performance and possibly lead to catastrophic aeroelastic instabilities (flutter).[1,2] Therefore, designing advanced aeroservoelastic control laws are an active area of reasearch as they are required to suppress these aeroelastic instabilities.[1,3,4,5,6]

Control-oriented, low order models are required to design and analyze such controllers. These simple models can be obtained either by model reduction of complex fluid/structure models[3,7] or using a flight dynamics approach.[8,9] In either case, a structural model of the aircraft is required, e.g. a finite element method (FEM) based model. Experimental data can be used to both validate and update such FEM models to ensure that they accurately model the actual aircraft structural dynamics.[10,11] The experiments to obtain such data should be designed aiming towards hte identification of the vibrational frequencies and mode shapes across a suitable frequency range.[12]

This paper focuses on Ground Vibration Test (GVT) procedures and post-processing algorithms to estimate modal frequencies and vibrational mode shapes. This builds on previous work done at the Uninhabited Aerial Vehicle (UAV) Laboratories at University of Minnesota (UMN).[13,14] The ground vibration tests described in 13, 14 were performed on the Body Freedom Flutter (BFF) vehicle developed by Lockheed Martin and the Air Force Research Lab.[4] This paper describes the application of similar GVT procedures to a series of aircraft, designed and built to study aeroelastic effects as part of a NASA project entitled 'Performance Adaptive Aeroelastic Wing' (PAAW). The updates in the GVT procedures include change in the type of excitation signal, a large increase in the sampling rate and the use of alternative post-processing algorithms. These updates and additional changes in the experimental procedure are described in details in this paper.

The remainder of the paper has the following outline. Section II provides details on the aircraft used for testing. This section also provides an overview of the related aeroelastic research project for which this aircraft was built. The GVT procedure is summarized in Section III. This section includes details about the experimental setup, data acquisition, and the experimental procedure. Section IV describes the post-processing required to estimate modal frequencies and mode shapes from the raw experimental data.

*Graduate Student, email: gupta165@umn.edu

†Assistant Professor, email: seile017@umn.edu

‡Principal Research Engineer, email: bdanowsky@systemstech.com

Two different approaches were applied: Quadrature response method[15] and Curve-fitting Frequency Domain Decomposition(CFDD).[16] These post-processing methods were applied to GVTs conducted on several similar airframes and the results are summarized in Section V. Finally, concluding remarks are provided in section VI.

II. Background

The UAV lab at the University of Minnesota conducts research in the field of aeroservoelasticity. Theoretical research is conducted on topics varying from modeling,[17,18] model reduction[19,20] and control design.[21,6] Experimental work[13,14,22] and flight tests are also conducted to support and validate the theoretical research. Researchers at the UAV lab are working as part of a large industry/academic team for a NASA grant entitled 'Performance Adaptive Aeroelastic Wing' (PAAW). The main research objective of the project is to demonstrate flutter suppression control and design active wing shaping techniques to optimize performance during flight. The details of the project can be found at www.paaw.net. The lab follows an open source policy and the experimental (flight and ground test) data, mathematical models and flight software generated for the project are freely available on the PAAW website.

A series of aircraft were built by the UAV lab at UMN to act as testbeds for the research conducted for the PAAW project. The first aircraft in this series is designated as 'mAEWing1'. Two different center-bodies and three wing-sets of varying flexibilities have been designed and built thus far. The aircraft exhibit a modular design. The wings and the center-body can be separated and used interchangeably. The wings have one rectangular spar as the main load carrying member. The aerodynamic shape is achieved by encasing the support structure with foam. Additional details on the design, build and test of these aircraft can be found in 23.

The discussion in this paper focuses on two aircraft configurations named 'Sköll'[a] and 'Hati'[b]. Both these configurations have the same dimensions and shape as shown in Figure 1. Therefore, the aerodynamic properties of the aircraft are similar. However, the aircraft differ slightly in their structural properties due to differences in the construction. Key properties for the two aircraft configurations are given in Table 1. The last two columns of this table contains the average structural properties of the wings like flexural rigidity (EI) and torsional rigidity (GJ). These structural properties are estimated from static tests conducted on the aircraft.[23]

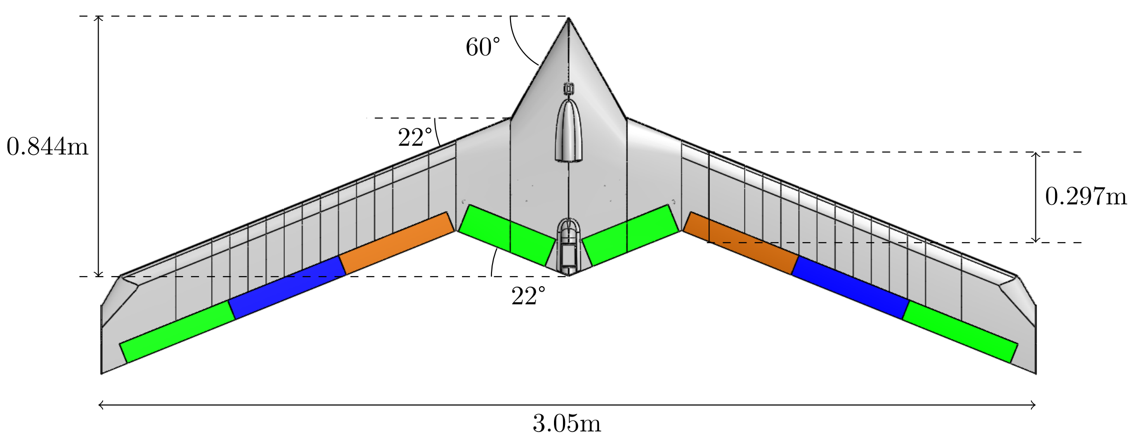

Figure 1. Aircraft dimensions

,

III. Experiment Details

The objective of the ground vibration test is to obtain the data which can be used to model the flexible dynamics of the aircraft. The aircraft is excited by an input force and accelerations are measured as outputs

[a] Sköll consists of center-body-1 and wing-set-1 of the mAEWing1 series of aircraft
[b] Hati consists of center-body-2 and wing-set-3 of the mAEWing1 series of aircraft

Table 1. **Key Aircraft Properties**

Aircraft	Mass (Kg)	CG Position (m)	Roll Inertia (Kg-m^2)	Pitch Inertia (Kg-m^2)	Yaw Inertia (Kg-m^2)	Wing EI (N-m^2)	Wing GJ (N-m^2)
Sköll	6.27	0.603	3.098	0.528	3.315	262.08	166.83
Hati	6.24	0.603	2.786	0.481	3.063	316.04	292.99

at multiple points across a grid on the aircraft. Several parameters of the experiment such as excitation location, accelerometer locations, type of the support of test aircraft, shaker attachment type and data acquisition frequency can be chosen based on the aircraft being tested. A detailed discussion of the general considerations that go into choosing these parameters are described in Ref. 12. The reasons behind the choice of these experimental parameters for the current GVT are described further below.

Ground vibration tests have been performed previously in the UAV lab at University of Minnesota on the Body Freedom Flutter aircraft developed by U.S. Air Force Research Laboratory and Lockheed Martin.[4] An HP35670A signal analyzer was used to generate the excitation signal as well as to directly compute the frequency response functions from the measured signal. The signal analyzer provided limited control over the excitation type and data acquisition parameters. The details of the previous experiment can be found in Ref. 13, 14. For the current GVT, a separate signal generator and data acquisition system is used. A detailed description of the setup used is given below.

A. Setup

The setup for the GVT is shown Figure 2. The photograph on the left shows Hati suspended from a wooden frame. The wooden frame provides the support structure for the test. The aircraft is suspended from the frame by a single flexible spring. The spring is chosen to be sufficiently flexible so as to approximate a free-free vibration condition. In particular, the spring has a stiffness of $k = 130\,\text{N/m}$ and the aircraft mass is approximately $m = 6.3\,\text{kg}$. Hence, the natural frequency of the mass/spring oscillation is $\sqrt{\frac{k}{m}} = 4.5\,\text{rad/sec} \approx 0.7\,\text{Hz}$. This is well below the expected fundamental vibration frequency of the aircraft which is around 5 Hz. Thus the mass/spring oscillation mode should not interfere with the identification of the flexible modes of the aircraft.[12]

The spring is attached to a metallic hook at the center of gravity (CG) of the aircraft. Attachment at the CG allows the aircraft to remain approximately horizontal throughout the test. In the previous GVTs,[13,14] the spring attachment was behind the CG and the aircraft hung more vertically. As a result, the excitation force provided perpendicular to the aircraft had a horizontal component. Therefore, the aircraft experienced some pendulum like rigid body vibrations in the previous GVTs. With the aircraft staying horizontal and the excitation force being applied in the vertical direction, any rigid body pendulum-like vibration is eliminated in the current GVT.

The excitation force can be provided to the aircraft in various forms. For example, an impulse force can be applied with an impact hammer. Alternatively, a shaker can be used to apply any specified excitation force, e.g. a discrete swept sine input or continuous chirp input. The impulse hammer provides only a single instantaneous excitation to excite all the frequencies while the excitation provided with a shaker persist for some time. Exciting the aircraft with a shaker averages out the noise in the measurement while using the hammer makes the measurement more prone to noise. Comparing the two common types of excitations provided by a shaker, a swept sine excitation is discrete and might not excite all the modes while a chirp excitation is continuous and is guaranteed to excite all the modes in it's frequency range. Therefore, a chirp input is chosen over the other excitations. This is an improvement over the previous GVT's[13,14] where swept sine input signals were used as signal analyzer was not capable of producing chirp signals. The photograph on the right in Figure 2 shows the shaker attached to one of the excitation point of Hati. An Unholz-Dickie Model 20 electrodynamic shaker is used to provide the excitation . The shaker can generate forces in excess of 1100 N and has a frequency range of 1–5000 Hz.

Experiments are conducted with symmetric excitation points on the longitudinal axis and unsymmetric points off this axis. These locations are shown in Figure 3. The excitation points are chosen away from the spar of the wings so that both bending and torsion modes are excited. One consideration that goes into choosing the excitation locations is artificial local stiffening due to the shaker attachment.[12] As both the attachment points are located on the stiff fuselage of the aircraft and not on the flexible wings, local stiffening does not enter into the picture for the current GVT.

The shaker is attached to the aircraft via a stinger and force transducer. First, a single-axis PCB-208C01 force transducer is attached to the excitation location on the aircraft using modeling clay or hot glue. This ensures that the surface of the aircraft does not get damaged while conducting the test. The force transducer is used to measure the actual force applied to the aircraft. It can measure both tensile and compressive forces. It operates in a frequency range of 0.01–36000 Hz and a magnitude range of ±44.5 N. Next, a stinger is attached between the force transducer and the shaker. The stinger is used to transmit only the perpendicular forces to the aircraft and reduce the transmission of any transverse forces. This is important for a complex structure like aircraft because transverse forces might interfere with the excitation of modes of interest like the bending and torsion modes. Using a stinger also ensures the force is only applied in the single axis measurable by the uni-axial force transducer.

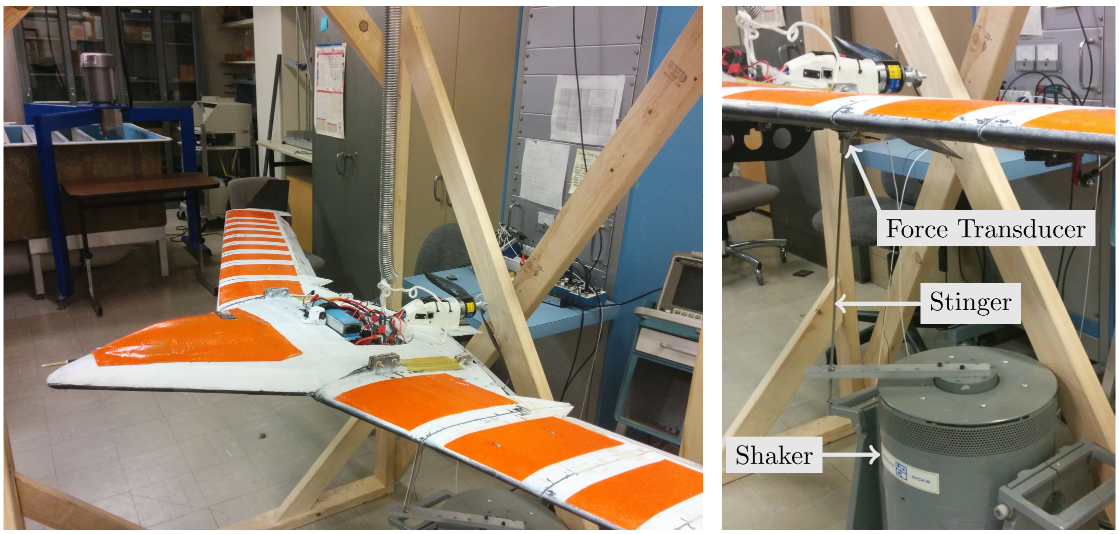

Figure 2. Setup for GVT: Suspended aircraft and shaker.

B. Data Acquisition

Figure 3 shows the grid of output locations at which the accelerations are measured in the GVTs. The grid points should be chosen such that all the modes can be captured. As the twenty points on the grid are located away from the spars and spread across the wings, the grid should be capable of capturing both the bending and the torsion modes. PCB-353B16 accelerometers are used to measure the response of the aircraft at these twenty locations. These sensors measure accelerations in the range of $\pm 500g$ (where g is acceleration due to gravity) and can operate in the frequency range of 1–10000 Hz. As recommended, a PCB-480E09 signal conditioner is used in both the accelerometer and force transducer measurement circuit. The signal conditioner has amplification settings of 1x, 10x and 100x. The force measurement is not amplified while the accelerometer measurements are amplified by 100x. A National Instrument NI9269 signal generator is used to generate the desired input signal to the electrodynamic shaker. It has a 16 bit resolution and can generate a voltage in the range of ±10 V. Finally, a National Instrument NI9229 data acquisition system is used to record various signals. It has 4 channels, a 24 bit resolution, and works with signals in the range of ±60 V. The data acquisition system logs the data at 2000 Hz. Note that this is a significant increase beyond the 70 Hz sample rate used in the previous experiments[13, 14] which was limited by the signal analyzer.

C. Procedure

As noted above, the data acquisition system has four channels. Two of these channels are used for the input signal to the shaker and the force transducer measurement. This leaves the remaining two channels for accelerometer measurements. Measurements at the twenty grid locations shown in Figure 3 are therefore collected in ten consecutive experiments. Accelerometers are placed at two grid locations for each experiment.

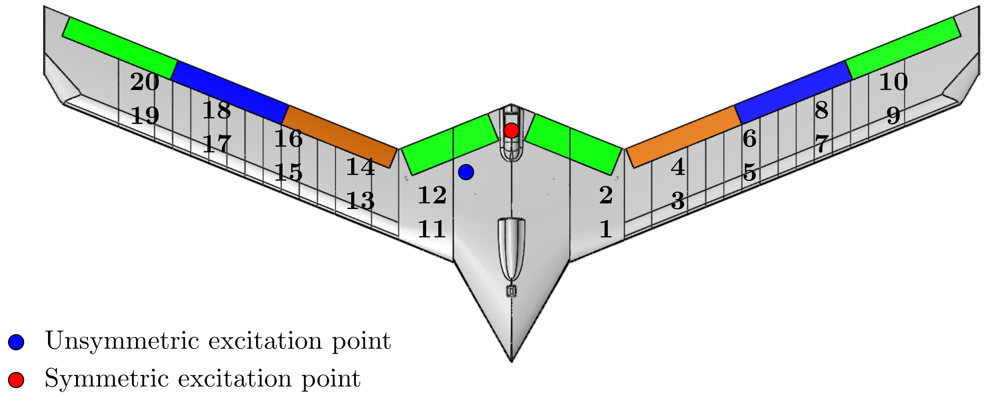

Figure 3. Excitation points and accelerometer grid point

The shaker input command is specified as a constant amplitude chirp input of the form $A\sin(\omega(t)t)$. The chirp frequency varies linearly with time, i.e. $\omega(t) = c_0 + c_1 t$. It is important to note that the shaker and the aircraft interact as a system. As a result, the actual force applied to the aircraft (and measured with the force transducer) does not have a constant amplitude throughout the experiment. At the beginning of each experiment the aircraft is allowed to vibrate for about 7 seconds before the data acquisition is started. This is done to ensure the aircraft vibration reaches steady state before any data is recorded. Initial GVTs on each aircraft are performed using a chirp frequency range from 3–35 Hz. Narrower frequency ranges are used for follow-up GVTs in order to identify modal frequencies and mode shapes more precisely. Narrowing the frequency range increases the amount of time for which a particular frequency window is excited. This results in a reduction in noise and therefore a more precise measurement. The duration of each experiment is approximately two minutes.

Each GVT, thus, consists of ten independent experiments, each yielding two accelerometer measurements and one force transducer measurement. The accelerometer and force transducer measurements are all sampled at 2000 Hz. As mentioned above, the excitation force will vary throughout the experiment and will also vary from experiment to experiment. In the previous experiments,[13,14] an HP35670A Dynamic Signal Analyzer was used to directly compute frequency response data from input force to output accelerometer. The new procedure described here collects the raw time domain data instead, using the NI9229 data acquisition system. The next section describes the process to estimate modal frequencies and mode shapes using this collection of raw (time-domain) experimental data.

IV. Post-Processing

Two different approaches are applied to obtain modal frequencies and mode shapes from the raw (time-domain) data: Quadrature response method[15] and Curve-fitting Frequency Domain Decomposition(CFDD).[16] Both approaches differ significantly from the eigensystem realization method[24] used in the previous GVTs[13,14] and are briefly summarized in this section.

As described previously, the GVT consists of ten experiments. Each experiment generates measurements of the input force f and two accelerometers (a_{m_1} and a_{m_2}) at a pair of locations (m_1, m_2). The collection of time domain samples for one experiment is thus $\{t_k, f(t_k), a_{m_1}(t_k), a_{m_2}(t_k)\}_{k=1}^{N}$. The peak picking approach used in quadrature response method requires this raw time domain data to be converted to the frequency domain. Specifically, the input force and accelerometer measurements are converted to the frequency domain via the Fast Fourier Transform (FFT). This conversion is done via the Matlab command `fft` and yields frequency domain data $\{\omega_k, F(j\omega_k), A_{m_1}(j\omega_k), A_{m_2}(j\omega_k)\}_{k=1}^{N}$. The frequency response from input force to output accelerometer at locations m_1 and m_2 on the aircraft structure are given by

$$G_{m_1}(j\omega_k) := \frac{A_{m_1}(j\omega_k)}{F(j\omega_k)} \text{ and } G_{m_2}(j\omega_k) := \frac{A_{m_2}(j\omega_k)}{F(j\omega_k)} \tag{1}$$

This calculation is repeated for each of the ten experiments to generate twenty frequency response functions

$\{G_m\}_{m=1}^{20}$ from the input force to the output acceleration at the locations shown in Figure 3.

The quadrature response method estimates modal frequencies using a 'sigma' plot. In this context, the maximum singular value from input force to the twenty accelerometer outputs is given by $\bar{\sigma}(G(j\omega)) := \sqrt{\sum_{m=1}^{20} |G_m(j\omega)|^2}$. Modal frequencies are identified by peaks on the 'sigma' plot of this maximum singular value versus frequency. Only modal frequencies in the 3–35 Hz range are identified as higher frequency vibrational modes are assumed to be irrelevant for aeroelastic control. The mode shapes are identified using the technique described by Stahle and Forlifer.[15] The quadrature response is the imaginary part of the frequency response function. Resonance occurs when the phase of the output measurement is ± 90 degrees out of phase with the input force. The amplitude of the mode at a particular point on the grid is given by the imaginary part of the frequency response function at that point for a specific modal frequency identified by the peak picking method. Theg specific approach to identify the mode shapes consists of the following steps. First, the Matlab command `fitfrd` is used to fit a transfer function to each to the twenty frequency response data. This fitting is done to smoothen the data and improve the quality of the estimated mode shapes. Next, the imaginary part of the transfer function at a particular identified modal frequency is computed for each of the twenty responses. This 20×1 vector is the estimated mode shape.

Note that the quadrature response at any frequency is the sum of the quadrature response due to different modes. The accuracy of the estimated mode shapes can be improved by taking these modal interactions into consideration. The procedure to do this is also provided in Ref. 15. This more accurate procedure was particularly useful for the GVT of previous aircraft[13, 14] which had closely spaced modes. This method is also applied to the current GVT. However, no significant improvement is observed and the results are similar to the simplified approach. This is because the modal frequencies for the current aircraft are sufficiently separated from each other. Therefore, the quadrature response at a particular modal frequency is predominantly due to the corresponding mode and therefore, the initial estimates of mode shape can be considered a suitable approximations of the actual mode shapes.

This quadrature response method can be sensitive to the noise in the GVT data. For example, consider a case where the noise in the measured data results in noise in the phase difference between the input force and the output acceleration for different output points. In this case, the calculated quadrature response, which depends on the measured phase at different grid points, will not represent the physical mode shapes. This phenomena is observed particularly for lower frequency modes.

The second approach discussed here is known as Curve-fitting Frequency Domain Decomposition (CFDD). The CFDD approach has been applied successfully to both simulated and actual flight test data in previous work.[16] The classical approach used to identify modal characteristics of a vibrating system is based on picking the peaks in the power-spectral density diagram.[25] This is the basis for the first approach described above. For well separated modes, the technique can give a reasonable estimation of natural frequencies and mode shapes. However when the modes are closely spaced, the estimation of the mode shapes and natural frequencies can become heavily biased.[26] Also, the autospectra of the output signals do not provide sufficient information to estimate accurate normal modes of vibration.[16] The cross-spectra magnitude and phase along with coherence are also equally important to provide an accurate estimation of the normal modes.

However, using classical frequency domain analysis for picking dominant peaks imposes a great deal of practical difficulties. All cross-spectral density plots need to be investigated and this becomes impractical when there are many measurements to deal with. To remedy this issue, Refs. 26, 27, suggested the use of the Singular Value Decomposition (SVD) of the power spectral-density matrix. In this approach, the power spectral-density matrix is first built from all measured outputs containing diagonal elements with the autospectral density of each output and off-diagonal elements with the cross-spectral densities of individual outputs. The power spectral-density matrix at each frequency of interest is then decomposed by applying SVD to the matrix. The Frequency Domain Decomposition theory states that the first singular vector corresponding to the first singular value is an estimate of the mode shape corresponding to a single degree of freedom system. With the identified autospectral density function, the natural frequencies and the damping ratios can easily be estimated. The CFDD technique is a method to directly identify the natural frequencies and the damping ratios from the Single Degrees of Freedom (SDOF) spectrum of measured outputs. As the name indicates, this method fits each SDOF spectrum with a second order transfer function and the roots of the denominator of the identified transfer function provides the estimation of the natural frequencies and the damping ratios of the individual SDOF vibration modes.

V. Results

A summary of the results obtained from the GVT conducted on two aircraft configurations described above are presented in this section. Both post-processing methods summarized in Section IV are used to identify modal frequencies and mode shapes.

A. Sköll

For the GVT on Sköll, the input excitation was provided at an unsymmetric excitation point. The force transducer was mounted using modeling clay. A GVT consisting of 10 experiments was conducted for the 20 grid-point locations. The target frequency range was set to 3–35 Hz. The time domain data was analyzed using both the quadrature response and CFDD methods. Both the methods gave similar results in terms of modal frequencies as shown in column 1–3 of Table 2. The mode shapes obtained from the two methods were also similar. The four mode shapes in the target frequency range, obtained using the quadrature response method are shown in Figure 4.

Table 2. Modal Frequencies of 'Sköll' configuration

Mode number	GVT-1 Frequencies(Hz)		GVT-2 Frequencies(Hz)	
	Quadrature Response	CFDD	Quadrature Response	CFDD
1	7.23	7.23	7.24	7.28
2	8.17	8.14	8.18	8.19
3	15.58	15.58	–	–
4	26.10	26.02	–	–

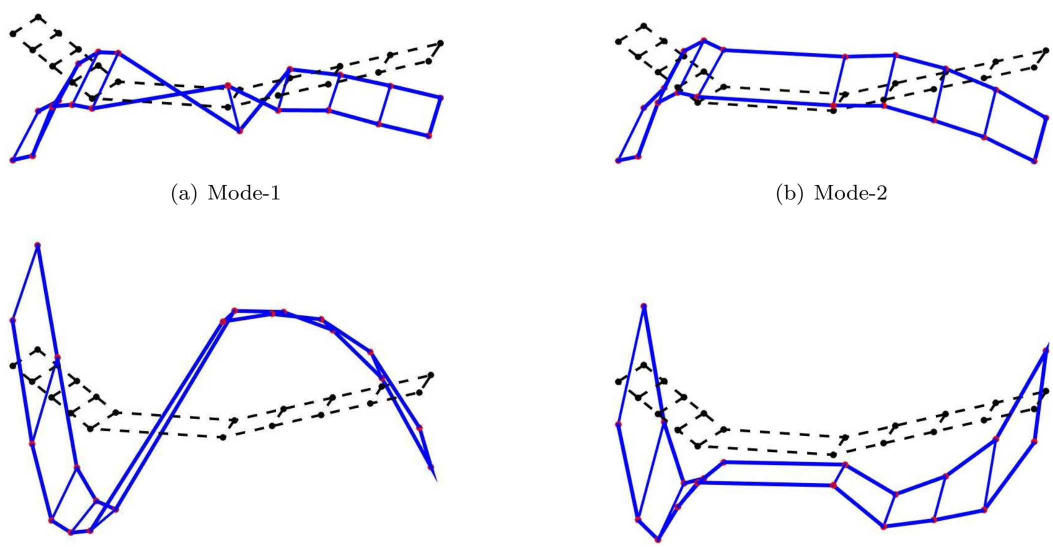

(a) Mode-1 (b) Mode-2 (c) Mode-3 (d) Mode-4

Figure 4. Mode shapes from quadrature response method: First GVT on Sköll

The identified mode shapes look like the basic symmetric and anti-symmetric bending modes as expected. The torsion mode could not be identified with these GVT data. It can also be seen that modal frequencies of Modes 1 and 2 are close to each other. The two corresponding mode shapes look similar to each other although the mode shape for the first mode seems to be more noisy.

Due on these results, a second GVT was conducted to resolve the first two mode shapes more clearly. The second GVT was again conducted using the unsymtretic excitation point with a series of 10 experiments, each taking two minutes. However, the frequency range of the chirp excitation was restricted to 3–13 Hz. This focus on the first two modes reduced the effect of noise in the mode shape estimate. The modal frequencies for the first two modes obtained from this GVT using both the methods are given in column 4–5 of Table 2. The modal frequencies only changed by a small amount as compared to the previous GVT.

The mode shapes obtained using the quadrature response method are shown in Figure 5. It can be seen that conducting a GVT with a lower range of target frequency helps in reducing noise in the mode shapes. But, it can also be observed that Mode 1 and 2 still seem to resemble the first symmetric bending modes. It is believed that these two modes might arise due to existence of asymmetry in the left/right wing stiffness. This asymmetry causes the first symmetric bending mode to split into the two closely spaced (in frequency) bending modes that are observed in the results from both the GVTs .

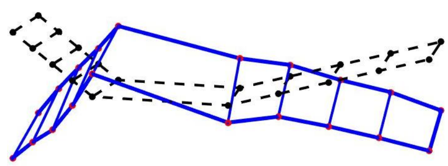

(a) Mode-1

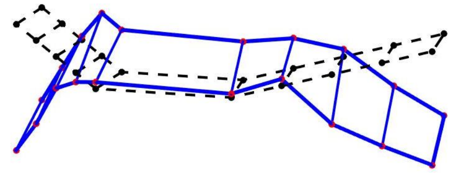

(b) Mode-2

Figure 5. Mode shapes from quadrature response method: Second GVT on Sköll

B. Hati

A few minor changes were made in the GVT procedure for Hati as compared to the GVT of the Sköll configuration. The force transducer was mounted on the aircraft using hot glue instead of modeling clay. The hot glue mount is more rigid compared clay mount. Hence, the force transfer was more efficient and resulted in less noise in the force measurement.

Two GVTs with different excitation points were conducted for the Hati configuration. The unsymmetric excitation point was used for the first GVT and the symmetric excitation point was used for the second GVT. The symmetric excitation in the second GVT was used to excite the symmetric modes more cleanly. Also, as the perpendicular separation between the spar location and the excitation point is increased. Hence, this second GVT excites the torsion modes with higher energy.

Both the quadrature response and CFDD methods were applied on the GVT data. While the CFDD method was able to identify 5 modes including the torsion mode, in the target frequency range of 3–35 Hz, the quadrature response method could not identify one of the bending modes (mode–2). The modal frequencies identified by both the methods are given in Table 3. It should be noted that for CFDD method, mode-4 was identified from the unsymmetric GVT while the other modes were identified from the symmetric GVT. The modes identified by the quadrature response method were all obtained from the symmetric GVT.

The first five mode shapes identified using the CFDD method are shown in Figure 6. It can be seen that due to the improvements made in GVT process, the mode shapes are less noisy in general compared to the one obtained for the Sköll configuration. Apart from the bending modes, the torsion mode (mode-3) was also excited with sufficient energy and was identified in this GVT.

Table 3. Modal Frequencies of 'Hati' configuration

Mode number	Modal Frequencies(Hz)	
	Quadrature Response	CFDD
1	7.95	7.96
2	–	13.83
3	15.96	15.97
4	19.22	19.07
5	32.0	31.9

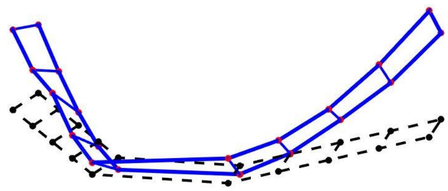

(a) Mode-1

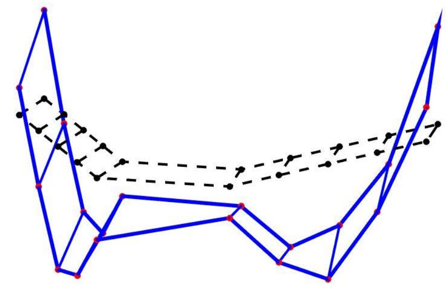

(b) Mode-2

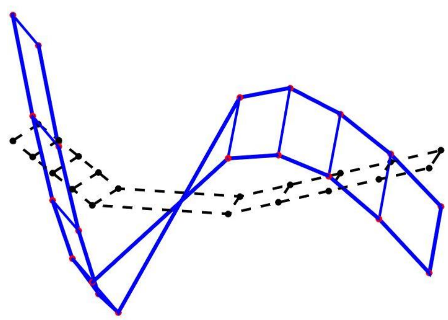

(c) Mode-3

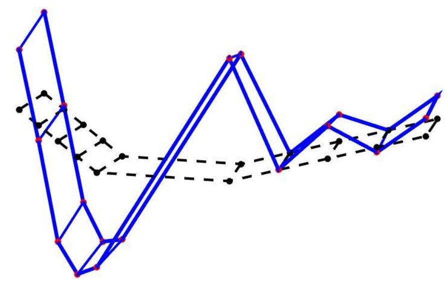

(d) Mode-4

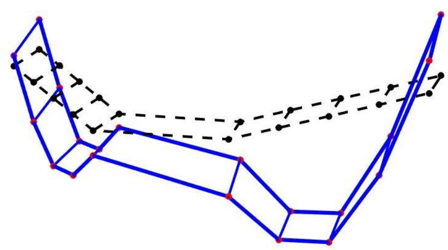

(e) Mode-5

Figure 6. Mode Shapes: Hati

VI. Conclusion

Ground vibration test were conducted on two aircraft configurations in the mAEWing1 series of aircraft. The experimental procedure is described. Two methods to obtain modal data from the experimental time domain data are discussed. The results of the GVT conducted on two aircraft are presented in the form of identified mode shapes and modal frequencies. It was found that for a given experiment duration, a high frequency range of the chirp excitation can adversely affect the noise in the identified modes, especially the modes in low frequency range. It was also found that torsion modes are difficult to excite and careful selection of excitation location is required to excite and identify these mode shapes. Small changes in the experimental procedures like using hot glue instead of modeling clay to mount force transducer, using different excitation points can make a significant difference in the identification of modal parameters.

VII. Acknowledgement

The authors acknowledge the NASA NRA NNX14AL36A, Lightweight Adaptive Aeroelastic Wing for Enhanced Performance Across the Flight Envelope, Mr. John Bosworth Technical Monitor, Mr. Dan Moerder acting Technical Monitor, for funding this research. The authors also acknowledge the PAAW research group for their continued support and suggestions which were critical in the success of the research.

References

[1]Beranek, J., Nicolai, L., Buonanno, M., Burnett, E., Atkinson, C., Holm-Hansen, B., and Flick, P., "Conceptual design of a multi-utility aeroelastic demonstrator," *13th AIAA/ISSMO Multidisciplinary Analysis Optimization Conference*, 2010, pp. 2194–2208.

[2]Lind, R. and Brenner, M., *Robust aeroservoelastic stability analysis*, Springer-Verlag, 1999.

[3]Danowsky, B. P., Thompson, P., Farhat, C., Lieu, T., Harris, C., and Lechniak, J., "Incorporation of Feedback Control into a High-Fidelity Aeroservoelastic Fighter Aircraft Model," *Journal of Aircraft*, Vol. 47, No. 4, 2010, pp. 1274–1282.

[4]Burnett, E., Atkinson, C., Beranek, J., Sibbitt, B., Holm-Hansen, B., and Nicolai, L., "NDOF Simulation model for flight control development with flight test correlation," *AIAA Modeling and Simulation Technologies Conference*, Vol. 3, 2010, pp. 7780–7794.

[5]Patil, M. J. and Hodges, D. H., "Flight dynamics of highly flexible flying wings," *Journal of Aircraft*, Vol. 43, No. 6, 2006, pp. 1790–1799.

[6]Theis, J., Pfifer, H., and Seiler, P., "Robust Control Design for Active Flutter Suppression," *AIAA SciTech*, 2016.

[7]Nguyen, N. and Tuzcu, I., "Flight dynamics of flexible aircraft with aeroelastic and inertial force interactions," *AIAA Atmospheric Flight Mechanics Conference*, Vol. 6045, 2009.

[8]Schmidt, D. K., *Modern Flight Dynamics*, McGraw Hill, 2012.

[9]Waszak, M. R. and Schmidt, D. K., "Flight dynamics of aeroelastic vehicles," *Journal of Aircraft*, Vol. 25, No. 6, 1988, pp. 563–571.

[10]Mottershead, J. E. and Friswell, M. I., "Model updating in structural dynamics: a survey," *Journal of sound and vibration*, Vol. 167, No. 2, 1993, pp. 347–375.

[11]Zárate, B. A. and Caicedo, J. M., "Finite element model updating: Multiple alternatives," *Engineering Structures*, Vol. 30, No. 12, 2008, pp. 3724–3730.

[12]Ewins, D. J., *Modal Testing: Theory and Practice*, Research Studies Press Ltd., 1984.

[13]Moreno, C. P., Gupta, A., Pfifer, H., Taylor, B., and Balas, G. J., "Structural model identification of a small flexible aircraft," *American Control Conference*, 2014, pp. 4379–4384.

[14]Moreno, C. P., *Linear, Parameter-Varying Control of Aeroservoelastic Systems*, Ph.D. thesis, University of Minnesota, 2015.

[15]Stahle, C. V. and Forlifer, W. R., "Ground Vibration Testing of Complex Structures," *Flight Flutter Testing Symposium*, 1958, pp. 83–90.

[16]Schulze, P. C., Thompson, P. M., Danowsky, B. P., Lee, D., and Harris, C., "System Identification and Modal Extraction from Response Data," *AIAA Atmospheric Flight Mechanics Conference*, 2013.

[17]Kotikalpudi, A., Pfifer, H., and Balas, G. J., "Unsteady Aerodynamics Modeling for a Flexible Unmanned Air Vehicle," *AIAA Atmospheric Flight Mechanics Conference*, 2015, p. 2854.

[18]Kotikalpudi, A., Moreno, C. P., Taylor, B., Pfifer, H., and Balas, G. J., "Low cost development of a nonlinear simulation for a flexible uninhabited air vehicle," *American Control Conference*, 2014, pp. 2029–2034.

[19]Moreno, C. P., Seiler, P., and Balas, G. J., "Linear parameter varying model reduction for aeroservoelastic systems," *AIAA Atmospheric Flight Mechanics Conference*, 2012, p. 4859.

[20]Theis, J., Takarics, B., Pfifer, H., Balas, G. J., and Werner, H., "Modal Matching for LPV Model Reduction of Aeroservoelastic Vehicles," *AIAA Science and Technology Forum*, 2015.

[21]Wang, S., Pfifer, H., and Seiler, P., "Robust synthesis for linear parameter varying systems using integral quadratic constraints," *IEEE Conference on Decision and Control*, 2014, pp. 4789–4794.

[22]Gupta, A., Moreno, C. P., Pfifer, H., and Balas, G. J., "Updating a finite element based structural model of a small flexible aircraft," *AIAA Science and Technology Forum*, 2015.

[23]Regan, C. and Taylor, B., "mAEWing1: Design, Build test," *AIAA SciTech*, 2016.

[24]Juang, J. N. and Pappa, R. S., "An eigensystem realization algorithm for modal parameter identification and model reduction," *Journal of guidance, control, and dynamics*, Vol. 8, No. 5, 1985, pp. 620–627.

[25]Bendat, J. S. and Piersol, A. G., *Engineering applications of correlation and spectral analysis*, John Wiley and Sons, 1980.

[26]Brincker, R., Zhang, L., and Andersen, P., "Modal identification from ambient responses using frequency domain decomposition," *International Modal Analysis Conference*, 2000.

[27]Brincker, R., Ventura, C., and Andersen, P., "Damping estimation by frequency domain decomposition," *International Modal Analysis Conference*, 2001, pp. 698–703.